

# CRAFT-LoRA: Content-Style Personalization via Rank-Constrained Adaptation and Training-Free Fusion

Yu Li<sup>1,2\*</sup> Yujun Cai<sup>3</sup> Chi Zhang<sup>1†</sup>

<sup>1</sup>AGI Lab, Westlake University <sup>2</sup>George Washington University <sup>3</sup>The University of Queensland  
yul@gwu.edu, chizhang@westlake.edu.cn

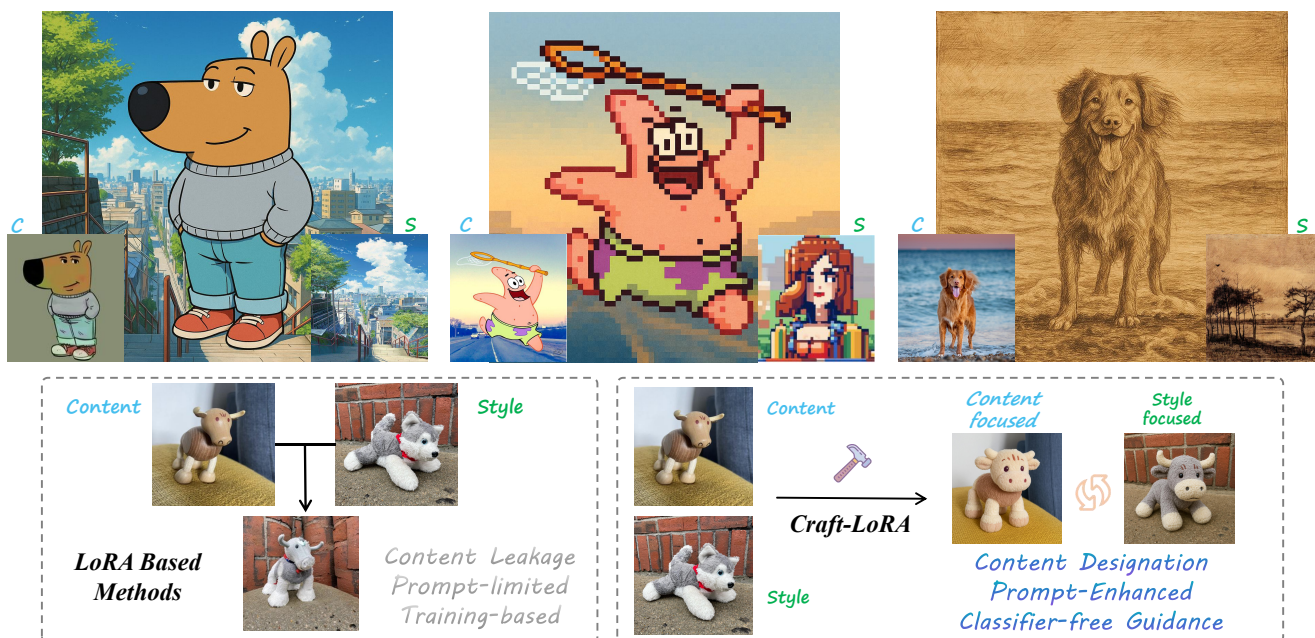


Figure 1. Samples generated by our proposed framework. Our method achieves more effective decoupling and fusion of content and style, enabling finer control over both aspects during generation.

## Abstract

Personalized image generation requires effectively balancing content fidelity with stylistic consistency when synthesizing images based on text and reference examples. Low-Rank Adaptation (LoRA) offers an efficient personalization approach, with potential for precise control through combining LoRA weights on different concepts. However, existing combination techniques face persistent challenges: entanglement between content and style representations, insufficient guidance for controlling elements’ influence, and unstable weight fusion that often require additional training. We address these limitations through **CRAFT-LoRA**, with complementary components: (1) rank-constrained backbone fine-tuning that injects low-rank projection residuals to encourage learning decoupled content and style subspaces; (2)

a prompt-guided approach featuring an expert encoder with specialized branches that enables semantic extension and precise control through selective adapter aggregation; and (3) a training-free, timestep-dependent classifier-free guidance scheme that enhances generation stability by strategically adjusting noise predictions across diffusion steps. Our method significantly improves content-style disentanglement, enables flexible semantic control over LoRA module combinations, and achieves high-fidelity generation without additional retraining overhead.

## 1. Introduction

Recent advancements in deep learning have fueled remarkable progress in generative models, particularly within personalized image generation [2, 11, 33]. Unlike generic image synthesis, personalized generation focuses on customizing

\*This work was done as a visiting student at AGI Lab.

†Corresponding author.

outputs based on user-provided references, such as a specific subject’s appearance or stylistic attributes, enabling applications in creative design, entertainment, digital avatars, and personalized marketing.

Among the various techniques developed for personalized image generation, Low-Rank Adaptation (LoRA) [15] has emerged as a particularly efficient approach by introducing small, trainable low-rank matrices into pre-trained text-to-image diffusion models, allowing fine-tuning on new concepts using only a small number of references. When integrated with frameworks like DreamBooth, LoRA-based methods enable customization to specific content or style from minimal examples [32]. Moreover, multiple independently trained LoRA modules can be simultaneously applied during inference, enabling images that blend diverse attributes such as combining a specific subject with a distinct artistic style. However, naively merging multiple LoRA modules often leads to degraded quality or semantic inconsistency due to entangled representations, motivating recent work on more effective fusion strategies [9, 25, 34].

Despite recent progress, existing LoRA combination strategies still face several fundamental challenges. First, although pre-trained diffusion models empirically exhibit some degree of composability with respect to LoRA modules, these models are not explicitly trained to support such combinations. As a result, directly merging LoRA weights often fails to achieve clean disentanglement between content and style factors [1, 20, 21]. Inspired by the meta-learning paradigm, particularly MAML [6, 8], which seeks optimal initializations for fast and generalizable task adaptation, we introduce a low-rank constrained adaptation phase inspired by PaRa [5] that narrows the model’s generative space to a more compact and disentangled representation that better supports multi-LoRA fusion.

Second, the notion of a subject in personalized image generation often encompasses a hierarchy of visual attributes, *e.g.* facial identity, hairstyle, clothing style, and accessory details. However, current methods typically collapse this rich semantic structure into a single coarse-grained token representation [22, 27], neglecting the internal structure of subject attributes and lacking mechanisms to control the preservation of fine-grained elements. To address this, we propose an expert encoder system with specially designed content and style adapters operating in disjoint network layers. The expert encoder processes identity labels, content descriptions, and style specifications through separate branches, facilitating selective aggregation based on semantic relevance and enabling fine-grained control over feature preservation at different levels.

Third, existing LoRA fusion strategies such as ZipLoRA [34] typically rely on additional optimization procedures to reconcile differences between LoRA modules [12, 41]. Directly modifying LoRA parameters during fusion can

inadvertently alter or suppress critical elements encoded in the original weights, leading to loss of identity or stylistic fidelity, while also incurring non-trivial computational overhead. To overcome these limitations, we propose a tuning-free asymmetric Classifier-Free Guidance (CFG) mechanism. Rather than adjusting LoRA weights directly, we selectively apply time-dependent modifications only to the conditional path while keeping the unconditional path anchored to base model weights, yielding a dynamic guidance signal that steers generation toward a desirable content-style balance without additional training cost.

As illustrated in Figure 2, our proposed unified framework integrates rank-constrained fine-tuning to learn decoupled content and style subspaces, leverages prompt-guided mechanisms for semantic control via selective adapter aggregation guided by an expert encoder, and employs a timestep-aware guidance correction scheme for stable, high-fidelity generation without extra training.

To summarize, we make the following key contributions:

- We propose a novel framework that enhances content-style disentanglement during LoRA training through rank-constrained fine-tuning and low-rank projection residuals, encouraging the learning of decoupled subspaces.
- We introduce a prompt-guided approach with an expert encoder and selective adapter aggregation, enabling precise semantic control over content and style influences and extending the applicability of LoRA modules.
- We develop a training-free time-step-aware and classifier-free guidance correction scheme that improves the stability and fidelity of diffusion-based generation by strategically adjusting noise predictions during critical steps.

## 2. Related Work

### 2.1. Personalized image generation

The research trajectory of image stylization has evolved from early Generative Adversarial Network-based domain translation methods—often relying on paired or unpaired datasets and extensive, domain-specific training—to diffusion-based frameworks [3, 4, 29]. More recently, the application of large pre-trained vision–language models has further advanced zero-shot editing and stylization. For instance, Prompt-to-Prompt [14] guides the generation process by selectively modulating cross-attention maps, while plug-and-play methods introduce lightweight adapters into self-attention layers to adjust spatial features dynamically [13, 23, 44]. Despite significant progress, reconciling high content fidelity with flexible style injection remains an open challenge [7, 17]. Practice shows that naive parameter fusion strategies, such as weighted averaging, often lead to unintended mixing of content and style features [36]. Consequently, current stylization pipelines often struggle to integrate diverse visual concepts without compromising either semantic coherence

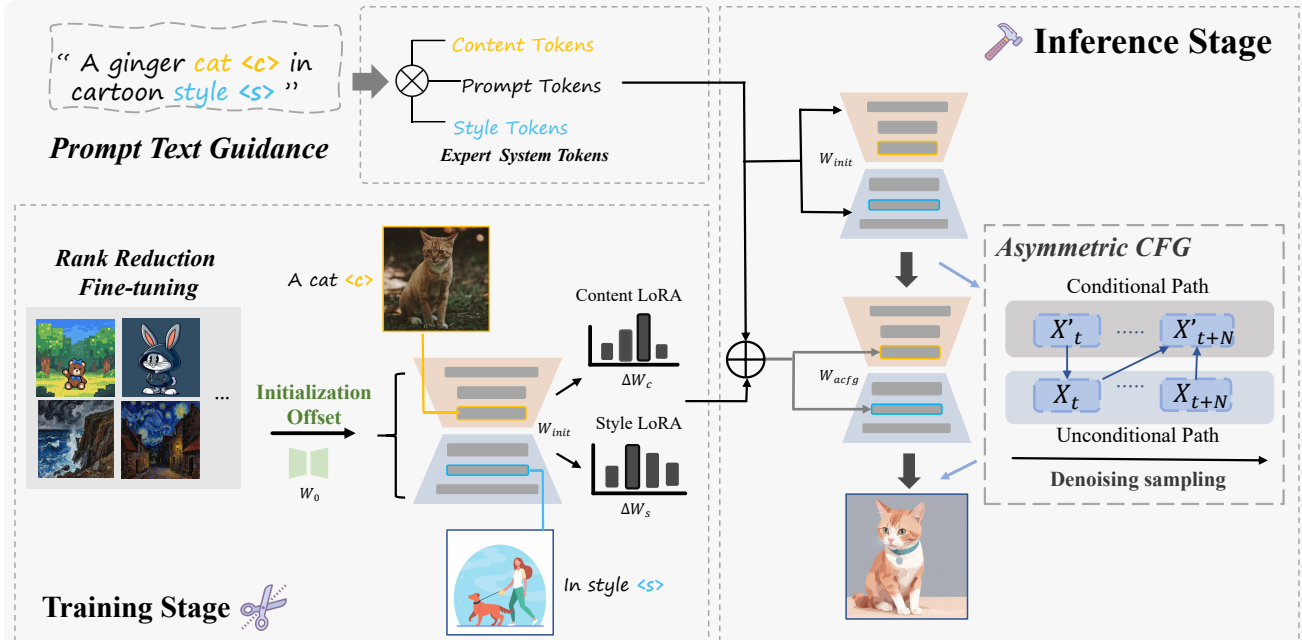


Figure 2. Overview of **CRAFT-LoRA**, a unified pipeline for personalized image synthesis. In the *Training Stage*, content ( $\Delta W_c$ ) and style ( $\Delta W_s$ ) LoRA adapters are decoupled from reference images using a rank-restricted initialization offset. The *Prompt Text Guidance* module employs an expert system with specialized branches to produce distinct content and style tokens for semantic control. In the *Inference Stage*, a timestep-aware asymmetric CFG scheme selectively integrates LoRA updates, ensuring stable and high-fidelity image generation.

or stylistic integrity [26, 39].

## 2.2. Fine-Tuning and LoRA Composition for Stylization

The rapid advancement of text-to-image diffusion models has spurred diverse personalization strategies. Full-model fine-tuning approaches such as DreamBooth [30] achieve high-fidelity transfer but incur substantial computational costs and require lengthy retraining on domain-specific examples. To mitigate these demands, Parameter-Efficient Fine-Tuning (PEFT) techniques have emerged [12, 31]. Among these, LoRA [15] introduces small, trainable low-rank decomposition matrices, injecting new stylistic or semantic concepts while keeping the majority of pre-trained weights frozen, thus striking a balance between adaptability and efficiency. Complementary approaches include token-based optimization techniques such as Textual Inversion [10], which learns new embeddings to represent novel concepts within the model’s token vocabulary, and adapter-based schemes such as StyleDrop [37], which appends lightweight layers to attention blocks to isolate style information in dedicated modules. Meta-learning, as a cross-task method for domain transfer, shares similar principles with style transfer in personalized image generation, providing new inspirations for fine-tuning methods [45].

A key challenge arises when combining multiple LoRA

modules for simultaneous content and style adaptation. Parameter interpolation [38, 40] provides a basic approach but is prone to suboptimal outcomes, especially when parameters conflict. To address this, several studies refine the composition mechanism: ZipLoRA [34] learns column-wise mixing coefficients for each content-style pairing, B-LoRA [9] differentiates functional roles within attention modules for content-style separation, and LoRA Composition [46] employs a cyclic update mechanism to iteratively guide generation without explicit parameter merging. Training-free approaches have also been explored, with K-LoRA [25] selectively applying LoRAs to different attention layers and CLoRA [24] proposing contrastive test-time composition. Other directions include QR-LoRA [43], which applies QR decomposition for parameter-efficient training, and LoRA.rar [35], which learns merging via hypernetworks. While these methods improve the merging or composition process, the upstream entanglement inherent in standard backbones remains underexplored.

## 3. Methodology

### 3.1. Preliminaries

LoRA is an efficient fine-tuning method that adapts pre-trained diffusion models by adding trainable low-rank matrices  $A \in \mathbb{R}^{r \times n}$  and  $B \in \mathbb{R}^{m \times r}$  to frozen weights  $W_0 \in$

$\mathbb{R}^{m \times n}$ , yielding  $W = W_0 + BA$  with  $r \ll \min(m, n)$ . In personalized image generation, content LoRAs  $\Delta W_c$  represent subject-specific features such as identity and structure, while style LoRAs  $\Delta W_s$  capture artistic aspects such as texture and color. Both can be trained efficiently from a single reference image, and during inference they can be composed into the backbone to produce personalized outputs.

### 3.2. Framework Overview

We propose **CRAFT-LoRA**, a unified framework for personalized image synthesis that addresses content-style disentanglement and fusion in LoRA-based methods. As shown in Fig. 2, the framework consists of three main stages: (1) *Training Stage*, where content and style LoRA weights are learned separately based on a rank-constrained fine-tuned backbone; (2) *Prompt Text Guidance*, which employs an expert encoder system with specialized branches to provide semantic control over content and style during training and inference; (3) *Inference Stage*, utilizing a timestep-aware asymmetric classifier-free guidance scheme for stable and flexible fusion of LoRA weights without extra training.

### 3.3. Rank-Limited Fine-Tuning of Backbone

As discussed in the introduction, pre-trained diffusion models do not explicitly support clear disentanglement of content and style factors when adapting weights from a reference image. Motivated by the adaptability of MAML [8, 18] under few-shot constraints and leveraging the rich hierarchical features of SDXL [28], we propose to fine-tune the U-Net backbone under a rank-constrained mechanism that provides optimized initialization and structurally improves content-style disentanglement for subsequent LoRA training.

**Rank Reduction Fine-Tuning.** Inspired by PaRa [5], we denote the frozen backbone weight matrix of layer  $l$  as  $W_l^{(0)} \in \mathbb{R}^{d_{\text{out}}^l \times d_{\text{in}}^l}$ , with  $L$  layers in total. We introduce a learnable basis matrix  $B_l \in \mathbb{R}^{d_{\text{in}}^l \times r_l}$  per layer, where  $r_l$  is the rank constraint satisfying  $r_l \ll \min(d_{\text{out}}^l, d_{\text{in}}^l)$ . Computing the QR decomposition  $B_l = Q_l R_l$  yields an orthonormal basis  $Q_l$  with  $Q_l^\top Q_l = I$ . The rank-limited fine-tuning projects out components of  $W_l^{(0)}$  along  $Q_l$ , yielding updated weights:

$$W_l = W_l^{(0)} - Q_l Q_l^\top W_l^{(0)}. \quad (1)$$

This operation constrains updates to directions orthogonal to the learned low-rank subspace, introducing an architectural bias that encourages reduced overlap between content and style representations. We show empirically in Appendix 5 that it reduces cross-influence.

To further allocate adaptation capacity hierarchically, we schedule:

$$r_l = r_{\text{max}} - \frac{l-1}{L-1}(r_{\text{max}} - r_{\text{min}}), \quad l = 1, \dots, L, \quad (2)$$

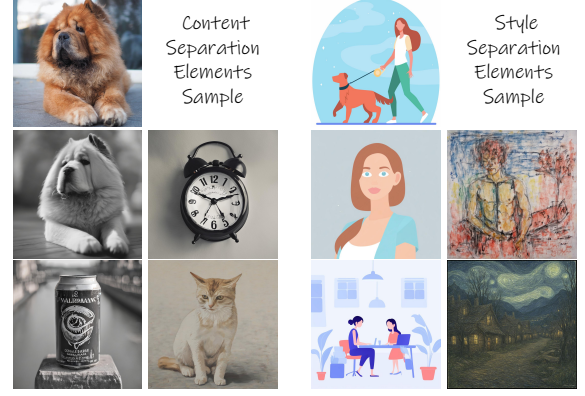


Figure 3. Content-style separation via frequency domain decomposition. Each group shows an original image with its frequency-separated elements and additional samples from the same group. Left: content group, where low-frequency components capture structural and semantic information. Right: style group, where high-frequency components capture textures and artistic rendering.

assigning higher ranks to earlier layers, which typically encode low-level structural and textural information where content and style factors are more intertwined, thus requiring more adaptation capacity. In implementation, we set  $r_{\text{max}} = 128$  and  $r_{\text{min}} = 4$ . Compared to a uniform rank  $r = 64$  across all layers, this schedule improves Content Similarity by 4.8%, Style Similarity by 5.2%, and reduces cross-influence by 11.3%, confirming the benefit of hierarchical rank allocation.

For content-style disentanglement, we train separate basis matrices  $B_l^{\text{content}}$  and  $B_l^{\text{style}}$ , obtaining corresponding orthonormal subspaces  $Q_l^{\text{content}}$  and  $Q_l^{\text{style}}$ . Merging these via concatenation and QR decomposition yields the combined weight update. Specifically, we first concatenate the basis matrices  $[B_l^{\text{content}} | B_l^{\text{style}}]$  and apply QR decomposition to their corresponding orthonormal subspaces:

$$Q_l^{\text{merged}} = [Q_l^{\text{content}} | Q_l^{\text{style}}] = Q_l^{\text{combined}} R_l^{\text{combined}} \quad (3)$$

$$W_l^{\text{combined}} = W_l^{(0)} - Q_l^{\text{combined}} (Q_l^{\text{combined}})^\top W_l^{(0)} \quad (4)$$

The fine-tuned backbone weights are retained to provide a targeted initialization, thereby empirically reducing the cross-influence between content and style factors. After rank-limited fine-tuning, we denote the resulting backbone as  $W_{\text{init}} = \{W_i^{\text{init}}\}_{i=1}^L$ , which serves as the host weights for all subsequent LoRA training and inference stages.

**Contrastive Content-Style Pairs.** To facilitate effective disentanglement during fine-tuning, we construct a curated dataset of 100 contrastive content-style image pairs. These pairs are designed so that either the content or the style remains constant while the other varies, guiding the model to separately capture content and style characteristics.

We operationalize the notion of content and style using frequency-domain decomposition: *content* corresponds primarily to low-frequency components encoding structural and semantic information such as object layouts, while *style* corresponds to high-frequency components capturing textures and color palettes. Specifically, we apply Gaussian low-pass filtering with cutoff frequency  $\sigma = 0.35$  (normalized) to extract content features, and compute the residual as style features. The cutoff was selected empirically by evaluating separation quality across  $\sigma \in \{0.2, 0.25, 0.3, 0.35, 0.4, 0.45, 0.5\}$  via MLLM-based assessment, with  $\sigma = 0.35$  yielding the best content-style separation across diverse reference images.

The content and style samples under this frequency method are shown in Figure 3. Concretely, we select 10 distinct content reference images  $\{C_i\}_{i=1}^{10}$  and 10 distinct style reference images  $\{S_j\}_{j=1}^{10}$ . Exhaustively pairing them yields:

$$\{(C_i, S_j) \mid i = 1, \dots, 10; j = 1, \dots, 10\}. \quad (5)$$

Fixing a content image  $C_1$  and combining it with styles  $\{S_1, \dots, S_{10}\}$  produces 10 pairs that vary only in style, while fixing a style and varying content produces complementary pairs.

These contrastive pairs are directly used to drive the rank-limited backbone training described above. For each pair, the two images are fed as separate inputs: one provides supervision for learning the content-specific basis  $B_l^{\text{content}}$ , while the other supervises the style-specific basis  $B_l^{\text{style}}$ . The corresponding orthonormal subspaces  $Q_l^{\text{content}}$  and  $Q_l^{\text{style}}$  are then merged, and the backbone is updated according to Eqs.3,4. In this way, the model allocates content and style variations to disjoint low-rank subspaces, ensuring that the backbone initialization  $W_l^{\text{combined}}$  encodes reduced interference between the two factors. We find that diversity matters more than quantity since 50 pairs already achieve 95% of full performance, while increasing to 200 pairs yields less than 2% additional improvement.

Empirically, combining rank-limited updates with contrastive pairs leads to a **12%** reduction in average CLIP-based content–style similarity, indicating that the learned features exhibit reduced cross-influence. As further demonstrated in Table 1(b), removing Rank-FT results in the largest performance drop among all components, quantitatively confirming its central role in disentanglement. Details on dataset construction and training settings are provided in Appendix 5.

### 3.4. Specialized Decoupling and Fusion

Building on the rank-limited backbone initialization, we introduce a prompt-guided framework to further separate content and style at the adapter level. During training, content and style LoRA updates are learned on disjoint layer subsets

with explicit prompt markers. At inference, an expert encoder routes prompt information to selectively activate these adapters, enabling flexible fusion and fine-grained control.

**Prompt-Guided Decoupling and Encoding.** Given a raw prompt  $p$  containing explicit markers for content and style, e.g.  $p = \text{“A photo of a person } \langle c \rangle \text{ smiling in a watercolor style } \langle s \rangle \text{”}$ , we treat these markers as routing signals to regulate LoRA module activation and to prevent leakage of content semantics into the style branch and vice versa. The prompt with markers removed is encoded by the SDXL text encoder to produce a unified semantic embedding:

$$e_{\text{sem}} = \text{SDXL\_Encoder}(p \setminus \{\langle c \rangle, \langle /c \rangle, \langle s \rangle, \langle /s \rangle\}), \quad (6)$$

where  $e_{\text{sem}} \in \mathbb{R}^d$  carries the overall semantics. Similarly, we extract content-specific embedding  $e_c$  and style-specific embedding  $e_s$  associated with  $\langle c \rangle$  and  $\langle s \rangle$  respectively, enabling isolated semantic guidance for each branch.

Following standard LoRA parametrization, each layer  $i$  is updated by low-rank matrices. To bias the network towards disentanglement, we allocate disjoint index sets  $I_c$  and  $I_s$ : lower and middle layers primarily capture structure and identity (content), while higher layers encode textures and rendering patterns (style). Content-specific matrices  $A_i^{(c)}$  and style-specific matrices  $A_i^{(s)}$  are trained with the semantic embedding, and updates are restricted as

$$\Delta W_i = \begin{cases} B_i A_i^{(c)}(e_{\text{sem}}), & i \in I_c, \\ B_i A_i^{(s)}(e_{\text{sem}}), & i \in I_s, \\ 0, & \text{otherwise,} \end{cases} \quad (7)$$

so that gradient updates are confined to designated subsets guided by markers, which biases the learned representations towards more independent content and style subspaces.

At inference, the Expert Encoder processes the prompt and produces control scalars  $\gamma_c, \gamma_s$  that regulate the strength of content and style adapters. By default,  $\gamma_c, \gamma_s \in \{0, 1\}$  are set based on marker presence, and users can also continuously adjust them within  $[0, 1]$  for fine-grained control over content and style intensity. The aggregated backbone at inference is then computed as

$$W^{\text{agg}} = W_{\text{init}} + \sum_{i \in I_c} E_i(\gamma_c \Delta W_i^{(c)}) + \sum_{i \in I_s} E_i(\gamma_s \Delta W_i^{(s)}), \quad (8)$$

where  $W_{\text{init}}$  denotes the rank-limited backbone obtained in Eqs.3,4. The operator  $E_i(\cdot)$  injects its input into the  $i$ -th layer while filling zeros elsewhere, so the summation operates as a layerwise direct sum.

If markers  $\langle c \rangle$  or  $\langle s \rangle$  are absent, the corresponding branch remains inactive. Users may also directly adjust  $\gamma_c, \gamma_s$  to control the relative influence of content and style, enabling flexible compositions such as “preserve content but

---

**Algorithm 1** Prompt-Guided Decoupling & Aggregation

---

**Input:** backbone  $W_{\text{init}}$ ; embeddings  $e_{\text{sem}}, e_c, e_s$ ; content/style scalars  $\gamma_c, \gamma_s$

**Output:** aggregated backbone  $W^{\text{agg}}$

- 1: Initialize updates  $\Delta W_i^{(c)} \leftarrow 0, \Delta W_i^{(s)} \leftarrow 0$  for all  $i$
  - 2: **for**  $i = 1 \rightarrow L$  **do**
  - 3:     **if**  $i \in I_c$  **then** update  $\Delta W_i^{(c)} \leftarrow B_i A_i^{(c)}(e_{\text{sem}})$
  - 4:     **else if**  $i \in I_s$  **then** update  $\Delta W_i^{(s)} \leftarrow B_i A_i^{(s)}(e_{\text{sem}})$
  - 5:     **end if**
  - 6: **end for**
  - 7: Compute  $W^{\text{agg}}$  as in Eq. (8)
  - 8: **return**  $W^{\text{agg}}$
- 

replace style” without retraining. The full inference procedure is summarized in Algorithm 1, showing how prompts route into disjoint LoRA branches and produce the aggregated backbone  $W^{\text{agg}}$ .

**Asymmetric Classifier-Free Guidance** In standard classifier-free guidance (CFG), the conditional and unconditional paths share the same model weights. When LoRA updates are applied, this causes the unconditional path to be contaminated by content and style adapters, leading to instability in image generation. To address this issue, we propose Asymmetric Classifier-Free Guidance (ACFG), where the conditional path uses LoRA-adapted weights while the unconditional path remains anchored to the rank-limited backbone  $W_{\text{init}}$ .

Let  $i \in \{1, \dots, L\}$  index model layers and  $t \in \{1, \dots, T\}$  diffusion timesteps. Instead of uniformly applying LoRA updates at all timesteps, we introduce time-dependent activation schedules  $\gamma_c(t) = \mathbb{1}_{t \in T_c}$  and  $\gamma_s(t) = \mathbb{1}_{t \in T_s}$ , where  $T_c$  and  $T_s$  denote the active timestep ranges for content and style respectively. In practice, we activate content LoRA during early-to-mid timesteps to establish structural layout, and style LoRA during mid-to-late timesteps to refine textures and rendering, reflecting the coarse-to-fine nature of the diffusion process. The conditional weights at timestep  $t$  are:

$$W^{\text{cond}}(t) = W_{\text{init}} + \sum_{i \in I_c} E_i(\gamma_c(t) \Delta W_i^{(c)}) + \sum_{i \in I_s} E_i(\gamma_s(t) \Delta W_i^{(s)}) \quad (9)$$

while the unconditional path uses only the initialization backbone throughout:

$$W_i^{\text{uncond}}(t) = W_i^{\text{init}}, \quad \forall t, i. \quad (10)$$

The conditional and unconditional noise predictions are  $\epsilon_{\text{cond}} = \epsilon_{\theta}(x_t | W^{\text{cond}}(t), \text{cond})$  and  $\epsilon_{\text{uncond}} = \epsilon_{\theta}(x_t | W^{\text{uncond}}, \emptyset)$  respectively. The final guided estimate is:

$$\epsilon_{\theta}^{\text{acfg}} = (1 + \omega) \epsilon_{\text{cond}} - \omega \epsilon_{\text{uncond}}, \quad (11)$$

---

**Algorithm 2** Asymmetric CFG (ACFG) Sampling

---

**Input:** backbone  $W_{\text{init}}$ ; LoRA updates  $\{\Delta W_i^{(c)}\}, \{\Delta W_i^{(s)}\}$ ; schedules  $T_c, T_s$ ; guidance  $\omega$

**Output:** final sample  $\hat{x}_0$

- 1: Initialize  $x_T \sim \mathcal{N}(0, I)$ ; **for**  $t = T \rightarrow 1$  **do**
  - 2:  $\gamma_c(t) \leftarrow \mathbb{1}_{t \in T_c}, \gamma_s(t) \leftarrow \mathbb{1}_{t \in T_s}$
  - 3: Build  $W^{\text{cond}}(t)$  as in Eq. (17); set  $W^{\text{uncond}} \leftarrow W_{\text{init}}$
  - 4: Compute  $\epsilon_{\text{cond}}, \epsilon_{\text{uncond}}$ ; form  $\epsilon_{\text{acfg}}$  as in Eq. (19)
  - 5:  $x_{t-1} \leftarrow \text{Denoise}(x_t, \epsilon_{\text{acfg}}, t)$
  - 6: **end for**
  - 7: **return**  $\hat{x}_0$
- 

where  $\omega$  controls guidance strength. The key insight is that by anchoring the unconditional path to  $W_{\text{init}}$ , the guidance signal  $\epsilon_{\text{cond}} - \epsilon_{\text{uncond}}$  isolates the effect of LoRA adapters at each timestep, rather than conflating adapter influence with the unconditional baseline. Combined with the time-dependent schedules, this allows content structure to be established before style details are applied, reducing interference between the two factors. Crucially, ACFG requires no additional training or parameter optimization and maintains the same two-pass computation as standard CFG. Therefore, ACFG can be directly applied to standard SDXL LoRAs as a single module without the rank-limited backbone, providing improved fusion stability albeit with reduced disentanglement.

## 4. Experiments and Results

### 4.1. Implementation Details

For content concepts, we use the DreamBooth dataset [30] (30 themes, 4-5 images each). Style concepts come from StyleDrop [37], supplemented with art style images. Each LoRA module is trained from a single reference image. We construct 100 contrastive pairs from these sources via frequency-domain decomposition to enhance content-style separation during backbone fine-tuning. For evaluation, we use strictly disjoint train/test splits. Each metric is averaged over 10 content-style pairs with 10 generated images per pair. Content and Style Similarity are computed using CLIP-I embeddings. The Combination Score follows MLLM-based binary judgment practices [19]: GPT-4o is presented with the content reference, style reference, and output, and asked whether the output successfully integrates both content identity and artistic style. The final score is the average success rate over 50 evaluations per sample.

All experiments use Stable Diffusion XL [28] on NVIDIA 4090 GPUs with DreamBooth training at rank  $r = 64$ , Adam-8bit optimizer, 1000 steps, and learning rate  $1 \times 10^{-5}$ . For rank-constrained backbone fine-tuning, we use  $r_{\text{max}} =$

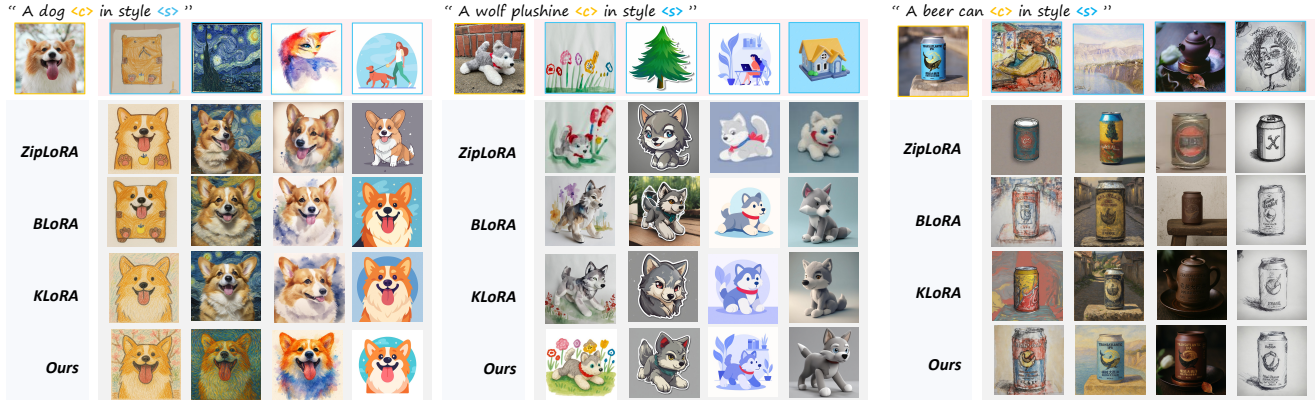


Figure 4. Visual comparison of content-style combinations. The figure presents a systematic evaluation of different methods in combining specific content elements with distinct artistic styles. Each column showcases the content and style reference followed by the outputs generated. Prompts follow the format “A [content] <c> in [style] <s>”. Competing methods often fail to simultaneously preserve structure and render style, whereas our method produces consistent and coherent content–style compositions.



Figure 5. Extended visual results. (a) Content–style generations augmented with additional prompt descriptions *e.g.* “catching a frisbee”, “wearing a hat”, and “driving a car”. Our method flexibly integrates dynamic semantics while preserving the specified content and style. (b) Single-branch generations where only the content LoRA or only the style LoRA is activated. Content-only generations preserve object identity across neutral renderings, while style-only generations transfer artistic features across different subjects.

128,  $r_{\min} = 4$  with linear decay, assigning higher ranks to earlier layers where content and style are more entangled. Compared to uniform rank  $r = 64$ , this schedule improves Content Similarity by 4.8% and Style Similarity by 5.2% while reducing cross-influence by 11.3%. This fine-tuning is a one-time cost of 5000 steps on  $2 \times 4090$  GPUs, after which  $W_{\text{init}}$  is reused for all subsequent LoRA training. During inference, ACFG maintains the same two-pass

structure as standard CFG with less than 5% additional overhead. For  $T = 50$  sampling steps, we set  $T_c = [1, 35]$  and  $T_s = [15, 50]$ , with an overlapping window allowing content and style to jointly influence the mid-stage transition.

## 4.2. Results and Analysis

In this section, we present a comprehensive analysis of our proposed method, encompassing visual demonstrations, quantitative evaluations against baselines, and an ablation study investigating the contributions of key components.

**Visual Results.** Figure 4 compares our method with representative LoRA fusion baselines, including ZipLoRA, BLoRA, and KLoRA. Prompts are formatted as “A [content] <c> in [style] <s>” with different content–style pairs such as dogs, plush toys, and objects. While existing methods often compromise either content fidelity *e.g.* structural distortion or style rendering *e.g.* muted patterns, our approach produces outputs that preserve object identity while faithfully capturing artistic styles. Figure 5 provides extended qualitative demonstrations. The top part shows content–style combinations augmented with additional prompt descriptions *e.g.* “catching a frisbee”, “playing with a ball”, or “driving a car”. Our method integrates these dynamic semantics while faithfully maintaining the designated content and style. The bottom part isolates the effect of single-branch adapters. Activating only the content branch preserves structural fidelity of objects across neutral renderings, while activating only the style branch applies stylistic transformations consistently across varied subjects. These observations confirm that our framework achieves effective disentanglement and controllability during inference.

**Quantitative Evaluation.** We evaluate our method using both automatic and human-centered metrics. For automatic evaluation, we adopt *Content Similarity* and *Style Similar-*

(a) Quantitative Comparison					
Method	Content Sim. (CLIP-I) $\uparrow$	Style Sim. (CLIP-I) $\uparrow$	Comb. Score (GPT-4o) $\uparrow$		
Direct Merging	0.65	0.60	0.62		
StyleDrop	0.68	0.76	0.70		
ZipLoRA	0.70	0.69	0.73		
KLoRA	0.71	0.72	0.76		
BLoRA	0.74	0.70	0.77		
LoRA.rar	0.73	0.71	0.76		
<b>Ours</b>	<b>0.79</b>	<b>0.80</b>	<b>0.83</b>		

(b) Component ablation study					
Rank-FT	Router	ACFG	Content Sim. $\uparrow$	Style Sim. $\uparrow$	Comb. Score $\uparrow$
			0.65	0.60	0.62
✓			0.73	0.70	0.72
	✓		0.69	0.65	0.67
		✓	0.68	0.64	0.66
✓	✓		0.76	0.76	0.80
✓		✓	0.75	0.73	0.78
	✓	✓	0.71	0.68	0.70
✓	✓	✓	<b>0.79</b>	<b>0.80</b>	<b>0.83</b>

(c) User Study			
Method	Content Fidelity $\uparrow$	Style Fidelity $\uparrow$	Coherence $\uparrow$
Direct Merging	2.3	2.0	2.1
StyleDrop	2.8	3.6	3.0
ZipLoRA	3.1	3.3	3.4
KLoRA	3.3	3.5	3.5
BLoRA	3.5	3.4	3.6
<b>Ours</b>	<b>4.1</b>	<b>4.3</b>	<b>4.4</b>

Table 1. Quantitative evaluation of our method. (a) Comparison against baselines using CLIP-I similarities and GPT-4o binary judgment scores. (b) Component ablation: Rank-FT contributes most to disentanglement, Router provides content-style routing, and ACFG stabilizes fusion; all three are complementary. The baseline (no components) corresponds to Direct Merging. (c) User study ratings on a 1–5 scale (30 participants, 50 samples).

ity based on CLIP-I embeddings, as well as a *Combination Score* derived from GPT-4o that measures the overall coherence of content–style integration. Each score is averaged over 10 distinct content–style pairs, with 10 generated images per pair. As shown in Table 1 (a), baseline methods exhibit different trade-offs: Direct Merging fails to preserve either content or style, StyleDrop emphasizes style at the expense of structure, and ZipLoRA, KLoRA, BLoRA, and LoRA.rar achieve more balanced results but remain limited in overall coherence. Our method consistently achieves the highest scores across all metrics, demonstrating its ability to preserve structural fidelity while maintaining faithful style transfer and coherent integration.

**Ablation and User Study.** Table 1 (b) presents a comprehensive component ablation. Among individual components, Rank-FT contributes most significantly, improving Content Sim. by +0.08 and Style Sim. by +0.10 over the baseline,

confirming its central role in content-style disentanglement. The Router provides complementary gains through layer-wise content-style routing, while ACFG stabilizes fusion quality. Combining any two components yields further improvements, and the full configuration achieves the best performance across all metrics, demonstrating that the three components are complementary.

Table 1 (c) reports results from a user study with 30 participants rating 50 samples on a 1–5 scale. Our method achieves the highest ratings across content fidelity, style fidelity, and overall coherence, consistent with the automatic metrics. This combination of quantitative and perceptual evidence confirms that our framework achieves superior disentanglement, fidelity, and integration compared with prior approaches.

**Failure Cases Analysis.** Despite the effectiveness of our approach, we identified three main failure modes during the diverse implementation process. First, when the reference image contains highly entangled content and style (*e.g.* a cartoon character whose identity is inseparable from the rendering), the method struggles to isolate content from style, resulting in style leakage into the content branch. Second, for styles dominated by low-frequency characteristics such as flat color palettes, the frequency-based separation misassigns these features to the content domain, leading to incomplete style capture. Third, abstract style descriptions (*e.g.* “ethereal mood”) may lack precise CLIP embeddings, resulting in weak or inconsistent style transfer. Adjusting the frequency cutoff  $\sigma$  or adopting stronger encoders could mitigate these issues.

## 5. Conclusion

We presented a framework for personalized image generation that integrates efficient adaptation strategies. Rank-constrained backbone fine-tuning encourages distinct subspaces, providing an inductive bias for disentanglement. An expert encoder with selective aggregation enhances semantic guidance, enabling flexible composition, and timestep-dependent asymmetric CFG introduces a training-free sampling strategy that improves visual quality. Our experiments demonstrate measurable reduction in content-style cross-influence, consistent improvements across automatic metrics, and clear user preference in perceptual studies. Limitations include architecture-dependent layer selection, reliance on text embedding quality, frequency-based separation assumptions that may not hold for flat textures, and the two-branch ACFG structure which limits multi-content or multi-style mixing. Standard SDXL LoRAs can be used with ACFG directly on the base model, though full disentanglement benefits require retraining on the fine-tuned backbone. Future work will explore automated layer assignment, multi-concept scheduling, and extensions to architectures such as KOALA [16] and SANA [42].

## Acknowledgement

This work was supported by the National Natural Science Foundation of China (No. 6250070674) and the Zhejiang Leading Innovative and Entrepreneur Team Introduction Program (2024R01007).

## References

- [1] Omri Avrahami, Kfir Aberman, Ohad Fried, Daniel Cohen-Or, and Dani Lischinski. Break-a-scene: Extracting multiple concepts from a single image. In *SIGGRAPH Asia 2023 Conference Papers*, pages 1–12, 2023. 2
- [2] Staphord Bengesi, Hoda El-Sayed, Md Kamruzzaman Sarker, Yao Houkpati, John Irungu, and Timothy Oladunni. Advances in generative ai: A comprehensive review of gans, gpt, autoencoders, diffusion model, and transformers. *IEEE Access*, 2024. 1
- [3] Andreas Blattmann, Robin Rombach, Huan Ling, Tim Dockhorn, Seung Wook Kim, Sanja Fidler, and Karsten Kreis. Align your latents: High-resolution video synthesis with latent diffusion models. In *Proceedings of the IEEE/CVF conference on computer vision and pattern recognition*, pages 22563–22575, 2023. 2
- [4] Zhipeng Cai, Zuobin Xiong, Honghui Xu, Peng Wang, Wei Li, and Yi Pan. Generative adversarial networks: A survey toward private and secure applications. *ACM Computing Surveys (CSUR)*, 54(6):1–38, 2021. 2
- [5] Shangyu Chen, Zizheng Pan, Jianfei Cai, and Dinh Phung. Para: Personalizing text-to-image diffusion via parameter rank reduction. *arXiv preprint arXiv:2406.05641*, 2024. 2, 4
- [6] Kurtland Chua, Qi Lei, and Jason D Lee. How fine-tuning allows for effective meta-learning. *Advances in Neural Information Processing Systems*, 34:8871–8884, 2021. 2
- [7] Jiwoo Chung, Sangeek Hyun, and Jae-Pil Heo. Style injection in diffusion: A training-free approach for adapting large-scale diffusion models for style transfer. In *Proceedings of the IEEE/CVF conference on computer vision and pattern recognition*, pages 8795–8805, 2024. 2
- [8] Chelsea Finn, Pieter Abbeel, and Sergey Levine. Model-agnostic meta-learning for fast adaptation of deep networks. In *International conference on machine learning*, pages 1126–1135. PMLR, 2017. 2, 4
- [9] Yarden Frenkel, Yael Vinker, Ariel Shamir, and Daniel Cohen-Or. Implicit style-content separation using b-lora. In *European Conference on Computer Vision*, pages 181–198. Springer, 2024. 2, 3
- [10] Rinon Gal, Yuval Alaluf, Yuval Atzmon, Or Patashnik, Amit H Bermano, Gal Chechik, and Daniel Cohen-Or. An image is worth one word: Personalizing text-to-image generation using textual inversion. *arXiv preprint arXiv:2208.01618*, 2022. 3
- [11] Isaias Ghebrehiwet, Nazar Zaki, Rafat Damseh, and Mohd Saberi Mohamad. Revolutionizing personalized medicine with generative ai: a systematic review. *Artificial Intelligence Review*, 57(5):128, 2024. 1
- [12] Zeyu Han, Chao Gao, Jinyang Liu, Jeff Zhang, and Sai Qian Zhang. Parameter-efficient fine-tuning for large models: A comprehensive survey. *arXiv preprint arXiv:2403.14608*, 2024. 2, 3
- [13] Shaozhe Hao, Kai Han, Shihao Zhao, and Kwan-Yee K Wong. Vico: Plug-and-play visual condition for personalized text-to-image generation. *arXiv preprint arXiv:2306.00971*, 2023. 2
- [14] Amir Hertz, Ron Mokady, Jay Tenenbaum, Kfir Aberman, Yael Pritch, and Daniel Cohen-Or. Prompt-to-prompt image editing with cross attention control. *arXiv preprint arXiv:2208.01626*, 2022. 2
- [15] Edward J Hu, Yelong Shen, Phillip Wallis, Zeyuan Allen-Zhu, Yuanzhi Li, Shean Wang, Lu Wang, Weizhu Chen, et al. Lora: Low-rank adaptation of large language models. *ICLR*, 1(2):3, 2022. 2, 3
- [16] Youngwan Lee, Kwanyong Park, Yoorhim Cho, Yong-Ju Lee, and Sung Ju Hwang. Koala: Empirical lessons toward memory-efficient and fast diffusion models for text-to-image synthesis. *Advances in Neural Information Processing Systems*, 37:51597–51633, 2024. 8
- [17] Yang Li, Songlin Yang, Wei Wang, and Jing Dong. Beyond inserting: Learning identity embedding for semantic-fidelity personalized diffusion generation. *arXiv preprint arXiv:2402.00631*, 2024. 2
- [18] Yu Li, Jin Huang, Yimin Zhang, Jingwen Deng, Jingwen Zhang, Lan Dong, Du Wang, Liye Mei, and Cheng Lei. Dual branch segment anything model-transformer fusion network for accurate breast ultrasound image segmentation. *Medical Physics*, 52(6):4108–4119, 2025. 4
- [19] Zhiqiu Lin, Deepak Pathak, Baiqi Li, Jiayao Li, Xide Xia, Graham Neubig, Pengchuan Zhang, and Deva Ramanan. Evaluating text-to-visual generation with image-to-text generation. In *European Conference on Computer Vision*, pages 366–384. Springer, 2024. 6
- [20] Chang Liu, Viraj Shah, Aiyu Cui, and Svetlana Lazebnik. Unziplora: Separating content and style from a single image. *arXiv preprint arXiv:2412.04465*, 2024. 2
- [21] Xiao Liu, Pedro Sanchez, Spyridon Thermos, Alison Q O’Neil, and Sotirios A Tsaftaris. Learning disentangled representations in the imaging domain. *Medical Image Analysis*, 80:102516, 2022. 2
- [22] Xihui Liu, Dong Huk Park, Samaneh Azadi, Gong Zhang, Arman Chopikyan, Yuxiao Hu, Humphrey Shi, Anna Rohrbach, and Trevor Darrell. More control for free! image synthesis with semantic diffusion guidance. In *Proceedings of the IEEE/CVF winter conference on applications of computer vision*, pages 289–299, 2023. 2
- [23] Pingchuan Ma, Xiaopei Yang, Yusong Li, Ming Gui, Felix Krause, Johannes Schusterbauer, and Björn Ommer. Scflow: Implicitly learning style and content disentanglement with flow models. In *Proceedings of the IEEE/CVF International Conference on Computer Vision*, pages 14919–14929, 2025. 2
- [24] Tuna Han Salih Meral, Enis Simsar, Federico Tombari, and Pinar Yanardag. Contrastive test-time composition of multiple lora models for image generation. In *Proceedings of the IEEE/CVF International Conference on Computer Vision*, pages 18090–18100, 2025. 3

- [25] Ziheng Ouyang, Zhen Li, and Qibin Hou. K-lora: Unlocking training-free fusion of any subject and style loras. *arXiv preprint arXiv:2502.18461*, 2025. 2, 3
- [26] Sang-Min Park and Young-Gab Kim. Visual language integration: A survey and open challenges. *Computer Science Review*, 48:100548, 2023. 3
- [27] Dario Pavllo, Aurelien Lucchi, and Thomas Hofmann. Controlling style and semantics in weakly-supervised image generation. In *Computer Vision—ECCV 2020: 16th European Conference, Glasgow, UK, August 23–28, 2020, Proceedings, Part VI 16*, pages 482–499. Springer, 2020. 2
- [28] Dustin Podell, Zion English, Kyle Lacey, Andreas Blattmann, Tim Dockhorn, Jonas Müller, Joe Penna, and Robin Rombach. Sdxl: Improving latent diffusion models for high-resolution image synthesis. *arXiv preprint arXiv:2307.01952*, 2023. 4, 6
- [29] Robin Rombach, Andreas Blattmann, Dominik Lorenz, Patrick Esser, and Björn Ommer. High-resolution image synthesis with latent diffusion models. In *Proceedings of the IEEE/CVF conference on computer vision and pattern recognition*, pages 10684–10695, 2022. 2
- [30] Nataniel Ruiz, Yuanzhen Li, Varun Jampani, Yael Pritch, Michael Rubinstein, and Kfir Aberman. Dreambooth: Fine tuning text-to-image diffusion models for subject-driven generation. In *Proceedings of the IEEE/CVF conference on computer vision and pattern recognition*, pages 22500–22510, 2023. 3, 6
- [31] Nataniel Ruiz, Yuanzhen Li, Varun Jampani, Wei Wei, Tingbo Hou, Yael Pritch, Neal Wadhwa, Michael Rubinstein, and Kfir Aberman. Hyperdreambooth: Hypernetworks for fast personalization of text-to-image models. In *Proceedings of the IEEE/CVF conference on computer vision and pattern recognition*, pages 6527–6536, 2024. 3
- [32] Simo Ryu. Low-rank adaptation for fast text-to-image diffusion fine-tuning. *Low-rank adaptation for fast text-to-image diffusion fine-tuning*, 3, 2023. 2
- [33] Sandeep Singh Sengar, Affan Bin Hasan, Sanjay Kumar, and Fiona Carroll. Generative artificial intelligence: a systematic review and applications. *Multimedia Tools and Applications*, pages 1–40, 2024. 1
- [34] Viraj Shah, Nataniel Ruiz, Forrester Cole, Erika Lu, Svetlana Lazebnik, Yuanzhen Li, and Varun Jampani. Ziplora: Any subject in any style by effectively merging loras. In *European Conference on Computer Vision*, pages 422–438. Springer, 2024. 2, 3
- [35] Donald Shenaj, Ondrej Bohdal, Mete Ozay, Pietro Zanuttigh, and Umberto Michieli. Lora. rar: Learning to merge loras via hypernetworks for subject-style conditioned image generation. In *Proceedings of the IEEE/CVF International Conference on Computer Vision*, pages 16132–16142, 2025. 3
- [36] Xincheng Shuai, Henghui Ding, Xingjun Ma, Rongcheng Tu, Yu-Gang Jiang, and Dacheng Tao. A survey of multimodal-guided image editing with text-to-image diffusion models. *arXiv preprint arXiv:2406.14555*, 2024. 2
- [37] Kihyuk Sohn, Lu Jiang, Jarred Barber, Kimin Lee, Nataniel Ruiz, Dilip Krishnan, Huiwen Chang, Yuanzhen Li, Irfan Essa, Michael Rubinstein, et al. Styledrop: Text-to-image synthesis of any style. *Advances in Neural Information Processing Systems*, 36:66860–66889, 2023. 3, 6
- [38] Anke Tang, Li Shen, Yong Luo, Yibing Zhan, Han Hu, Bo Du, Yixin Chen, and Dacheng Tao. Parameter efficient multi-task model fusion with partial linearization. *arXiv preprint arXiv:2310.04742*, 2023. 3
- [39] Maham Tanveer, Yizhi Wang, Ali Mahdavi-Amiri, and Hao Zhang. Ds-fusion: Artistic typography via discriminated and stylized diffusion. In *Proceedings of the IEEE/CVF International Conference on Computer Vision*, pages 374–384, 2023. 3
- [40] Hanqing Wang, Bowen Ping, Shuo Wang, Xu Han, Yun Chen, Zhiyuan Liu, and Maosong Sun. Lora-flow: Dynamic lora fusion for large language models in generative tasks. *arXiv preprint arXiv:2402.11455*, 2024. 3
- [41] Luping Wang, Sheng Chen, Linnan Jiang, Shu Pan, Runze Cai, Sen Yang, and Fei Yang. Parameter-efficient fine-tuning in large models: A survey of methodologies. *arXiv preprint arXiv:2410.19878*, 2024. 2
- [42] Enze Xie, Junsong Chen, Junyu Chen, Han Cai, Haotian Tang, Yujun Lin, Zhekai Zhang, Muyang Li, Ligeng Zhu, Yao Lu, et al. Sana: Efficient high-resolution image synthesis with linear diffusion transformers. *arXiv preprint arXiv:2410.10629*, 2024. 8
- [43] Jiahui Yang, Yongjia Ma, Donglin Di, Jianxun Cui, Hao Li, Wei Chen, Yan Xie, Xun Yang, and Wangmeng Zuo. Qr-lora: Efficient and disentangled fine-tuning via qr decomposition for customized generation. In *Proceedings of the IEEE/CVF International Conference on Computer Vision*, pages 17587–17597, 2025. 3
- [44] Yiming Zhang, Zhening Xing, Yanhong Zeng, Youqing Fang, and Kai Chen. Pia: Your personalized image animator via plug-and-play modules in text-to-image models. In *Proceedings of the IEEE/CVF conference on computer vision and pattern recognition*, pages 7747–7756, 2024. 2
- [45] Mandi Zhao, Pieter Abbeel, and Stephen James. On the effectiveness of fine-tuning versus meta-reinforcement learning. *Advances in neural information processing systems*, 35: 26519–26531, 2022. 3
- [46] Ming Zhong, Yelong Shen, Shuohang Wang, Yadong Lu, Yizhu Jiao, Siru Ouyang, Donghan Yu, Jiawei Han, and Weizhu Chen. Multi-lora composition for image generation. *arXiv preprint arXiv:2402.16843*, 2024. 3

# CRAFT-LoRA: Content-Style Personalization via Rank-Constrained Adaptation and Training-Free Fusion

## Supplementary Material

### Appendix

#### A. Trunk (Backbone) Fine-tuning Details

##### A.1. Targeted Dataset Construction

We construct a dataset of 100 content–style contrast pairs,  $\mathcal{D} = \{(I_c^k, I_s^k)\}_{k=1}^{100}$ . This dataset is used to fine-tune the backbone, encouraging content–style disentanglement and providing the base weights ( $W_{\text{init}}$ ) for subsequent LoRA adapter training. The pairs are generated using a pre-trained diffusion model with frequency-based controls.

For each pair  $(I_c^k, I_s^k) \in \mathcal{D}$ : image  $I_c^k$  emphasizes content, guided by a content prompt  $P_c^k$  and a style modifier  $P_{sm}^k$ ; image  $I_s^k$  emphasizes style, guided by a style prompt  $P_s^k$  and a content modifier  $P_{cm}^k$ . One specific  $P_{sm}^k$  and one  $P_{cm}^k$  are chosen per pair to form a one-to-one contrast.

We employ frequency-domain manipulations during iterative denoising. Let  $\mathcal{F}$  denote a frequency transform (e.g., Discrete Cosine Transform) and  $\mathcal{F}^{-1}$  its inverse. Masks  $\mathcal{M}_{\text{low}}$  and  $\mathcal{M}_{\text{high}}$  preserve low- and high-frequency components, respectively. With noisy latent  $z_t$  at timestep  $t$  and text embedding  $e = \text{TextualEmbeddings}(P)$ , the process is:

$$\begin{aligned} \hat{z}_0 &= \text{Predictor}(z_t, t, e), \quad (\text{Predict clean latent}) \\ z_{t-1}^{\text{filtered}} &= \mathcal{F}^{-1}(\mathcal{M}_{\text{low}} \odot \mathcal{F}(\hat{z}_0)) \quad (\text{for } I_c^k \text{ generation}), \\ z_{t-1}^{\text{filtered}} &= \mathcal{F}^{-1}(\mathcal{M}_{\text{high}} \odot \mathcal{F}(\hat{z}_0)) \quad (\text{for } I_s^k \text{ generation}), \\ z_{t-1} &= \text{UpdateRule}(z_t, z_{t-1}^{\text{filtered}}, \dots), \end{aligned}$$

where  $\odot$  denotes element-wise multiplication. This design concentrates variation along the intended factor (content or style).

Table 2. Conceptual illustration of content–style contrast pair generation. For each pair  $(I_c^k, I_s^k)$ , one varying modifier is chosen for  $I_c^k$  and one for  $I_s^k$ .

Property	$I_c^k$ (content fixed)	$I_s^k$ (style fixed)
Target image	Generated with fixed content	Generated with fixed style
Base prompt	$P_c^k$ : "a red car"	$P_s^k$ : "in the style of Van Gogh"
Varying modifier	$P_{sm}^k \in \{\text{watercolor, oil painting, } \dots\}$	$P_{cm}^k \in \{\text{starry night, sunflower, } \dots\}$
Dominant frequency filter	Low $\mathcal{M}_{\text{low}}$	High $\mathcal{M}_{\text{high}}$
Resulting characteristic	Content preserved with varied textures	Style preserved with varied subjects

##### A.2. Training Settings

We fine-tune the backbone weights  $\{W_l\}_{l=1}^L$  by minimizing:

$$\mathcal{L}_{\text{trunk}} = \mathcal{L}_{\text{task}}(\{W_l\}, \mathcal{D}) + \lambda_{\text{reg}} \sum_{l=1}^L \|B_l\|_F^2, \quad (12)$$

where  $B_l$  is a learnable basis for each layer  $l$ . Let  $B_l = Q_l R_l$  be the QR decomposition of the basis, where  $Q_l$  contains the orthonormal vectors ( $Q_l^\top Q_l = I$ ). Consistent with the update rule discussed in the main text, the weights are updated as:

$$W_l = W_l^{(0)} - Q_l Q_l^\top W_l^{(0)}. \quad (13)$$

This update effectively projects the original weights  $W_l^{(0)}$  onto the orthogonal complement of the learned subspace  $\text{span}(Q_l)$ . We denote the resulting post-finetuning backbone as  $W_{\text{init}}$  (also written  $\widetilde{W}$  in figures). The update  $\Delta W_l = -Q_l Q_l^\top W_l^{(0)}$  lies in  $\text{span}(Q_l)$ .

The per-layer rank  $r_l$  for the basis  $B_l$  follows a linear schedule:

$$r_l = r_{\text{max}} - \frac{l-1}{L-1} (r_{\text{max}} - r_{\text{min}}), \quad l = 1, \dots, L, \quad (14)$$

with maximum rank  $r_{\text{max}} = 128$  and minimum rank  $r_{\text{min}} = 4$ .

The task loss  $\mathcal{L}_{\text{task}}$  (Eq. 15) is computed over the dataset  $\mathcal{D}$ . Here,  $N = 100$ ,  $G(\cdot)$  represents the  $\hat{x}_0$  predictor (i.e., the U-Net),  $t$  is a sampled timestep, and  $z_t$  is the corresponding noisy latent created from the target image.

The perceptual term  $\mathcal{L}_{\text{perceptual}}$  (Eq. 16) is defined as: where  $\phi_j$  are features from VGG-19 (relu1\_1 to relu5\_1) and  $M_j$  is the number of elements in the feature map. We set  $\alpha = 0.1$  and  $\lambda_{\text{reg}} = 1 \times 10^{-4}$ .

Optimization uses the AdamW optimizer with a cosine decay learning rate schedule and a 500-step warm-up. The learning rate starts at  $1 \times 10^{-5}$ , warms up from  $1 \times 10^{-6}$ , and decays to a minimum of  $1 \times 10^{-7}$ . We use a batch size of 8 and train for 5000 steps.

## B. LoRA Training and Inference Details

### B.1. Setting and Notation

LoRA adapters are trained on the U-Net backbone initialized with the pre-tuned weights  $W_{\text{init}}$  (from Eq. 13). We define disjoint sets of U-Net layers  $I_c$  (for content) and  $I_s$  (for style), satisfying  $I_c \cap I_s = \emptyset$ . The adapters are trained only on the layers specified in  $I_c \cup I_s$ .

$$\mathcal{L}_{\text{task}}(\{W_l\}, \mathcal{D}) = \frac{1}{N} \sum_{k=1}^N \mathbb{E}_{t, z_t} \left[ \left\| G(\{W_l\}, z_t, t, \text{TextualEmbeddings}(P_c^k, P_{sm}^k)) - I_c^k \right\|_1 \right. \\ \left. + \left\| G(\{W_l\}, z_t, t, \text{TextualEmbeddings}(P_{cm}^k, P_s^k)) - I_s^k \right\|_1 \right] + \alpha \mathcal{L}_{\text{perceptual}}(\{W_l\}, \mathcal{D}). \quad (15)$$

$$\mathcal{L}_{\text{perceptual}} = \frac{1}{N} \sum_{k=1}^N \mathbb{E}_{t, z_t} \sum_{j \in \text{VGG\_layers}} \frac{1}{M_j} \left[ \left\| \phi_j(G(\{W_l\}, z_t, t, \text{TextualEmbeddings}(P_c^k, P_{sm}^k))) - \phi_j(I_c^k) \right\|_1 \right. \\ \left. + \left\| \phi_j(G(\{W_l\}, z_t, t, \text{TextualEmbeddings}(P_{cm}^k, P_s^k))) - \phi_j(I_s^k) \right\|_1 \right]. \quad (16)$$

Table 3. Summary of backbone fine-tuning hyperparameters.

Parameter	Value
Optimizer	AdamW
Initial learning rate	$1 \times 10^{-5}$
LR schedule	Cosine decay with 500 warm-up steps
Minimum learning rate	$1 \times 10^{-7}$
Batch size	8
Optimization steps	5000
Tuned U-Net layers	Attention and standard convolutional layers
Rank schedule $r_l$ (Eq. 14)	Linear; $r_{\max} = 128$ , $r_{\min} = 4$
$\mathcal{L}_{\text{task}}$ components	$\ell_1$ + Perceptual (VGG-19 relu1_1 to relu5_1)
Perceptual loss weight $\alpha$	0.1
$B_l$ regularization $\lambda_{\text{reg}}$	$1 \times 10^{-4}$
Hardware	2 NVIDIA 4090 GPUs

**LoRA parameterization.** For any layer  $i \in I_c \cup I_s$ , we use a fixed LoRA rank  $r = 16$ . Content adapters learn parameters  $\{B_i^{(c)}, A_i^{(c)}\}$  for  $i \in I_c$ ; style adapters learn parameters  $\{B_i^{(s)}, A_i^{(s)}\}$  for  $i \in I_s$ . The update is  $\Delta W_i = B_i A_i$ .

**Training procedure.** During content adapter training, gradients for  $\{B_i^{(c)}, A_i^{(c)}\}$  are enabled only for  $i \in I_c$  (and masked for  $i \in I_s$ ). Conversely, style adapter training only updates parameters for  $i \in I_s$ . Training hyperparameters are listed in Table 4. The specific layer assignments for content and style are shown in Table 5.

**Expert encoder and aggregation.** Three MLP encoders,  $E_t, E_c, E_s$ , produce 64-dimensional embeddings from a concept ID embedding, a CLIP content text embedding, and a CLIP style text embedding, respectively. Their concatenated features are fed into an aggregation head that outputs nonnegative scaling factors  $(\gamma_c, \gamma_s)$ . At inference, the aggregated

Table 4. LoRA adapter training hyperparameters.

Parameter	Value
Optimizer	AdamW
Learning rate	$1 \times 10^{-5}$
Training steps	1000–2000
Batch size	1
Backbone host	$W_{\text{init}}$ (from Eq. 13)

weights are:

$$W^{\text{agg}} = W_{\text{init}} + \sum_{i \in I_c} E_i(\gamma_c \Delta W_i^{(c)}) + \sum_{i \in I_s} E_i(\gamma_s \Delta W_i^{(s)}),$$

where  $E_i(\cdot)$  is an operator that injects the low-rank update  $\Delta W_i = B_i A_i$  at layer  $i$ .

## B.2. Disentanglement Metrics and Results

## B.3. Semantic Extension Examples

## C. Asymmetric Classifier-Free Guidance (ACFG) for Timestep-Dependent Aggregation

We introduce Asymmetric Classifier-Free Guidance (ACFG) during the sampling process. In ACFG, the conditional branch (guidance-seeking) uses the dynamically aggregated LoRA weights, while the unconditional branch (guidance-free) always uses the static, pre-tuned backbone initialization  $W_{\text{init}}$ .

**Conditional weights.** For timestep  $t \in \{1, \dots, T\}$ , the weights for layer  $i$  are:

$$W_i^{\text{cond}}(t) = W_{\text{init}, i} + \gamma_c(t) \Delta W_i^{(c)} + \gamma_s(t) \Delta W_i^{(s)}, \quad (17)$$

Table 5. U-Net layer assignments for content ( $I_c$ ) and style ( $I_s$ ) adapters.

Content layers ( $I_c$ )	Style layers ( $I_s$ )
down_blocks.2.attentions.0;	down_blocks.0.attentions.0;
mid_block.attentions.0;	down_blocks.1.resnets.0;
up_blocks.0.attentions.1;	mid_block.resnets.1;
up_blocks.1.attentions.0;	down_blocks.0.resnets.1;
up_blocks.2.attentions.0	down_blocks.1.attentions.1

content-style loras combination with given prompts

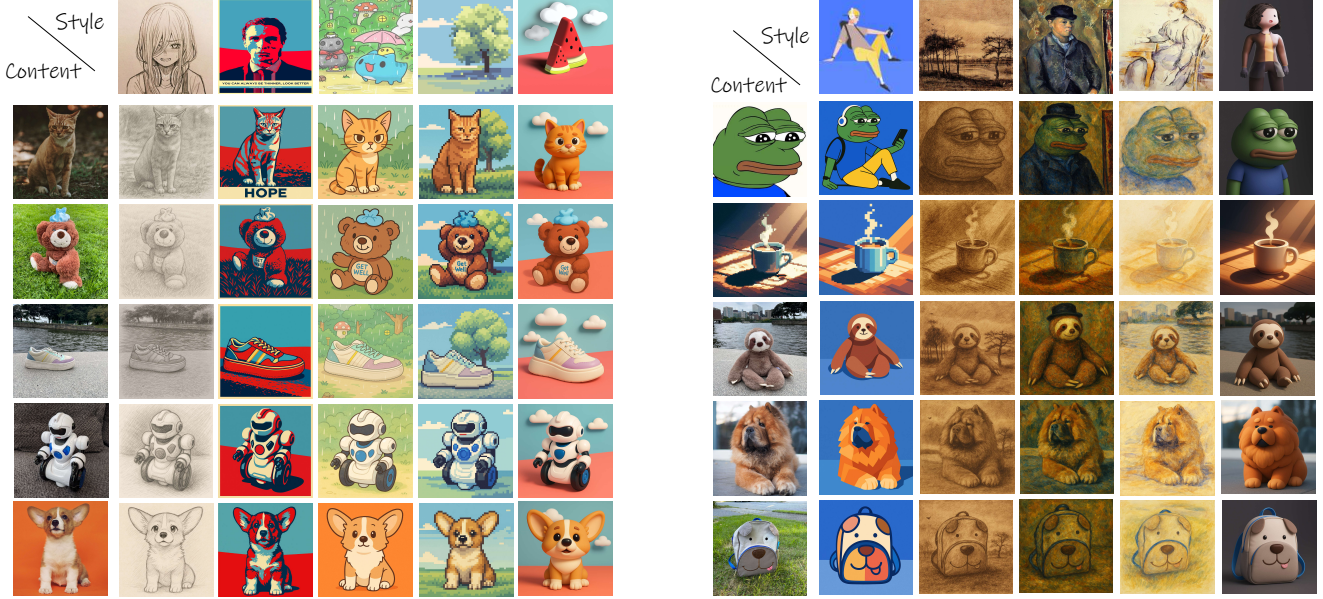


Figure 6. Visual results demonstrating content and style adapter performance.

Table 6. Disentanglement evaluation metrics.  $\mathcal{G}(p_c, p_s)$  denotes the final image generated from content prompt  $p_c$  and style prompt  $p_s$ . Higher is better for  $\mathcal{S}_c, \mathcal{S}_s$ ; lower is better for  $\mathcal{S}_x$ .

Metric	Formula	Description
Content preservation $\mathcal{S}_c$	$\frac{1}{N_s} \sum_{j=1}^{N_s} \text{sim}_c(\mathcal{G}(p'_c, p'_s{}^j), p'_c)$	Similarity to target content
Style fidelity $\mathcal{S}_s$	$\frac{1}{N_c} \sum_{i=1}^{N_c} \text{sim}_s(\mathcal{G}(p_c^i, p'_s), p'_s)$	Similarity to target style
Cross-influence $\mathcal{S}_x$	$\frac{1}{N_c N_s} \sum_{i,j} \text{interference}(p_c^i, p'_s{}^j)$	Undesired cross effect

where  $\gamma_c(t), \gamma_s(t) \geq 0$  are dynamic schedules (which can be binary or continuous). The unconditional weights are fixed:

$$W_i^{\text{uncond}}(t) = W_{\text{init},i} \quad \forall i, t. \quad (18)$$

Table 7. Quantitative comparison of content–style disentanglement.

Method	$\mathcal{S}_c \uparrow$	$\mathcal{S}_s \uparrow$	$\mathcal{S}_x \downarrow$
Standard LoRA	0.75	0.70	0.42
Trunk fine-tune + layer-selective LoRA (Ours)	<b>0.90</b>	<b>0.88</b>	<b>0.18</b>

Table 8. Types of semantic extension (generalization).

Type	Condition	Description
I	$p'_c \neq p_c^i, p'_s = p_s^j$	New content, trained style
II	$p'_c = p_c^i, p'_s \neq p_s^j$	Trained content, new style
III	$p'_c \neq p_c^i, p'_s \neq p_s^j$	New content, new style

**Guided prediction.** Let  $\epsilon_{\text{cond}} = \epsilon_{\theta}(x_t \mid \{W_i^{\text{cond}}(t)\}, \text{cond})$  be the noise estimate using conditional weights and  $\epsilon_{\text{uncond}} = \epsilon_{\theta}(x_t \mid \{W_i^{\text{uncond}}(t)\}, \emptyset)$  be the estimate using unconditional weights. The final ACFG

Table 9. Semantic extension examples via prompt variation.

Trained content	Trained style	Inference prompts	Type
“a red car”	“Van Gogh style”	$p'_c$ : “a blue car”, $p'_s$ : “Van Gogh style”	I
“a red car”	“Van Gogh style”	$p'_c$ : “a red car”, $p'_s$ : “sketch style”	II
“a red car”	“Van Gogh style”	$p'_c$ : “a bicycle”, $p'_s$ : “sketch style”	III
“person ID X”	“pixel art”	$p'_c$ : “person ID Y”, $p'_s$ : “pixel art”	I
“person ID X”	“pixel art”	$p'_c$ : “person ID X”, $p'_s$ : “cyberpunk style”	II

prediction is:

$$\epsilon_{\theta}^{\text{acfg}}(t) = (1 + \omega) \epsilon_{\text{cond}} - \omega \epsilon_{\text{uncond}}. \quad (19)$$

where  $\omega$  is the guidance scale.

**Zero-shot temporal scaling.** We propose a smooth schedule

$$\alpha(t) = \alpha_{\min} + (\alpha_{\max} - \alpha_{\min}) g\left(\frac{T - t}{T}\right),$$

with a monotone function  $g : [0, 1] \rightarrow [0, 1]$  (e.g., a cosine schedule). This  $\alpha(t)$  modulates the aggregation weights  $\gamma_c(t)$  and  $\gamma_s(t)$  to emphasize content early in the sampling (high  $t$ ) and refine style later (low  $t$ ), while always keeping the unconditional branch fixed as in Eq. 18.

Table 10. Performance by content–style pairing with ACFG. Metric shown is a composite quality score (higher is better).

Content–style pairing	Fixed-weights baseline	ACFG (ours)	Relative improvement
Similar semantics	0.81	0.87	+7.4%
Distant semantics	0.68	0.79	+16.2%
Complex composition	0.65	0.80	+23.1%

Table 11. Ablation of ACFG components. Higher indicates better quality.

Component configuration	Quality score	Relative change
Full ACFG as proposed	0.86	Reference
Constant temporal scaling (no time dependence)	0.78	−9.3%
No low-rank constraint on temporal adjustments	0.82	−4.7%
Standard CFG (uncond. path uses cond. weights)	0.75	−12.8%

## D. Additional Visualizations

Figures 6 and 7 provide additional qualitative results, complementing the visualizations in the main paper. These examples cover diverse objects, complex scenes, and challenging artistic styles, further demonstrating the robustness of our method. We also include failure cases to illustrate current limitations, such as difficulty with highly abstract styles or extreme compositional changes.



Examples of the emphasis requirements on content and style

A dog <c> in <s> style

B - LoRA



A dog <c> in <s> style, focusing on content/style elements

Ours



Examples of the textual reference extension

(Following previous results) A dog <c> is playing a ball / is driving a car / is cooking a meal in style <s>

B - LoRA



Ours



Figure 7. Additional visual results, including ACFG comparisons and semantic extensions.